Experimental study on K-joints of Concrete-Filled Steel Tubular truss structures

Wenjin Huang, Fujian Agriculture and Forestry University, Fuzhou (China)
Luigi Fenu[*]**,** University of Cagliari, Cagliari, Italy
Baochun Chen, Fuzhou University, Fuzhou (China)
Bruno Briseghella, Fuzhou University, Fuzhou (China)

Abstract

The failure modes of K-joints of Concrete Filled Steel Tubular (CFST) truss structures were investigated through laboratory tests. CFST K-joint specimens consisted of a tubular chord filled with concrete and two braces inclined at the same angle with respect to the chord. Their size was chosen of the same scale as that of joints of real tubular structures currently used in bridges. The results were compared with those obtained by testing K-joint specimens of Circular Hollow Section (CHS) truss structures with the same size. Contrary to CHS K-joints, where a chord face failure mode occurred, in CFST K-joints no failure mode with inward deformation of the chord section can occur. Hence, punching shear failure was shown to be the typical failure mode of CFST K-joints, if no brace failure mode occurred before. Resistance of CFST K-joints to punching shear was then compared with the resistance values calculated through the Eurocode 3 and the AWS code formulae on CHS K-joints. The values provided by the former formula were quite close to (although always lower than) the actual resistance to punching shear of CFST K-joints. Finally, the favourable effect on joint resistance due to additional studs welded to the interior surface of the chord tube of CFST K-joint was also investigated.

DOI: https://doi.org/10.1016/j.jcsr.2015.01.023
Article published in: Journal of Constructional Steel Research Volume 107, April 2015, Pages 182-193

Keywords

Tubular structures, CFST, truss, joint, failure mode, resistance

*** Corresponding Author**: Luigi Fenu, Department of Civil Engineering, Environment Engineering and Architecture. Piazza d'Armi, 09100 Cagliari, Italy.
Tel: +39 0706755434. Fax: +39 0706755418. E-Mail: lfenu@unica.it

1. Introduction

Currently, Concrete-Filled Steel Tubular (CFST) structures are frequently used in construction, especially in certain countries of Eastern Asia and especially in China [1-4].

In addition to wide use in both western and eastern countries to increase the load-bearing capacity of columns in tall buildings [5], in certain eastern countries, particularly in China, the technique of filling steel tubular structures with concrete also has been adopted in the arch trusses of many arch bridges [2], as well as in the truss girders of buildings and bridge decks. In bridges, CFST truss girders were first adopted in 1997 in the deck of the Zidong cable-stayed bridge in Nanhai City (Guangdong Province, China) [6]. Usually only the chords of CFST truss structures are filled with concrete, while the braces are not filled [2].

The strength and buckling resistances of chord members in compression are both considerably increased by the in-filled concrete. Han et al. showed that the concrete filling of the chords of curved built-up members subjected to axial compression was very effective in increasing their load-bearing capacity, initial stiffness and ductility [7]. Xue et al. studied the effect of debonding on the ultimate load-bearing capacity of CFST stub columns [8].

In CFST truss structures, thin-walled chord tubes with small wall thicknesses are commonly used [9]. Because they serve as an effective and useful formwork for concrete, their lightness greatly reduces difficulties in erecting truss-arch bridges, especially across deep valleys [1].

Welded joints are commonly used to connect the chord and brace members of both Circular Hollow Section (CHS) structures and CFST structures. In both cases, the connection is obtained by means of a butt or fillet weld along the entire perimeter of the end section of the brace. Therefore, the joints of CFST structures (CFST joints) differ from the joints of CHS structures (CHS joints) only in the concrete filling of the chords, which significantly affects the behaviour of CFST joints.

Compared with CHS joints [10-13], the scientific research on the behaviour and resistance of CFST joints is much less developed despite the increasing use of CFST truss structures.

A preliminary study on CFST joints dates back to the research of Tebbett et al [14], although its purpose was to investigate how to reinforce CHS joints rather than to investigate the resistance of CFST joints. Over a decade later, the work by Packer et al [15-18] highlighted the increased resistance due to the concrete fill in the chords of the tubular joints, and the CFST joints were shown to display different failure modes with respect to CHS joints.

Feng and Young studied the ultimate load-bearing capacity of CFST T-joints [19], while Han et al [20] and Zheng et al [21] investigated CFST N-joints, in particular the latter considered not only the chords but also the braces filled with concrete. Moreover, Chen [22] studied the effect of infilled grout on the static behaviour of tubular X-joints through testing large-scale joint specimens and developing a modeling procedure for FE analyses that can include the crack initiation and failure mode in the chord. The effect of lateral local compression on the CFST chord due to the compression brace was investigated by Hou et al [23-24]. Sakai et al [25] tested concrete-filled and reinforced tubular K-joints in truss girders by carrying out static and fatigue testing, thus finding that the fatigue strength of CFST joints is higher than that of CHS joints. The behaviour of CFST trusses (both curved and straight) was investigated by Xu et al [26] that, besides analysing the different failure modes of CFST trusses, noted that the effect of core concrete on joint failure was not significant when weld failure and chord punching shear failure were observed in tensile joints. The ultimate behaviour of the CFST joints in truss girders was also investigated by Huang [27] and Huang et al [28-29], and compared to that of CHS joints of truss girders with same geometry.

Nevertheless, additional experimental investigation is required to understand the behaviour and propose a reliable design method of the joints of such types of tubular structures.

In this paper, the resistance and failure modes of CFST K-joints were investigated using tests on real-size joints, with chord and brace members of the same scale as those used in the arch trusses and truss girders in many real bridges [30]. Also, the failure modes of CFST K-joints and CHS K-joints of the same size were compared. Moreover, the favourable effect on the behaviour of CFST joints due to welding studs on the interior surface of the chord member in the joint region was

investigated. Finally, the possibility of using the formulas proposed by the AWS code [31] and the Eurocode 3 [32] for CHS K-joints to assess the CFST K-joints was studied.

2. Test specimens and test set-up

In this work, CHS and CFST K-joint specimens were tested (Fig.1). These joints (together with the KT joints that function similarly to K-joints and are considered as K-joints by certain codes [33,34]) are the most common type of joint used in tubular girders and in the arch trusses of bridges.

The geometry of the K-joint specimens under consideration is described in Fig. 2. Two brace members (one in tension and the other in compression) were connected with a vertical chord member in compression. Both brace members were inclined at an angle of 60° to the chord, and their centrelines met each other along the vertical centreline of the chord member, thus no eccentricity existed (Fig. 2). Fillet welds were adopted for the welded connection between the brace and chord members, and their legs were twice the wall thickness of the brace. A DC (Direct Current) manual welding process was used.

Fig.1: View of a K-joint specimen and of the test set-up

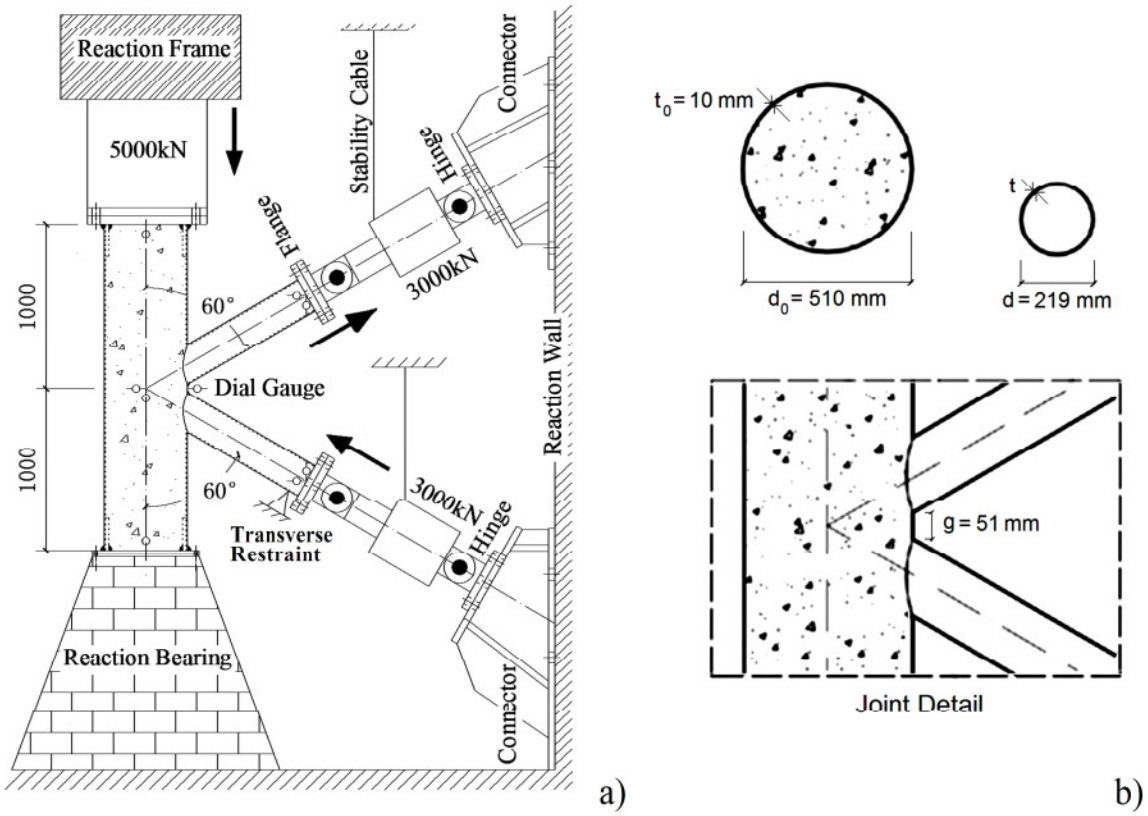

Fig. 2: Test set-up (a) and detail of specimen geometry (b)

The lengths of the chord and brace members were l_0 = 2000 and l = 900 mm, respectively. The chord sections of both CHS and CFST K-joint specimens were cold-formed and welded from a hot-rolled steel sheet with the same thickness, as used in the manufacturing of the chord tubes in real bridges. The outer diameter and thickness were d_0 = 510 mm and t_0 = 10 mm, respectively. The

Table 1. Size of the members of the K-joint specimens

K-joint specimens	d (mm)	t (mm)	l (mm)	d_0 (mm)	t_0 (mm)	L (mm)	θ (deg)	g (mm)	d/d_0	$d_0/(2t_0)$	t/t_0
CHS-6	219.0	6.0	900.0	510.0	10.0	2000.0	60°	51	0.43	25.5	0.60
CHS-8	219.0	8.0	900.0	510.0	10.0	2000.0	60°	51	0.43	25.5	0.80
CFST-6	219.0	6.0	900.0	510.0	10.0	2000.0	60°	51	0.43	25.5	0.60
CFST-8	219.0	8.0	900.0	510.0	10.0	2000.0	60°	51	0.43	25.5	0.80
CFST-10	219.0	10.0	900.0	510.0	10.0	2000.0	60°	51	0.43	25.5	1.00
CFST-6s *	219.0	6.0	900.0	510.0	10.0	2000.0	60°	51	0.43	25.5	0.60
CFST-8s *	219.0	8.0	900.0	510.0	10.0	2000.0	60°	51	0.43	25.5	0.80
CFST-10s *	219.0	10.0	900.0	510.0	10.0	2000.0	60°	51	0.43	25.5	1.00

*s = with studs

brace members (thickness t = 6 mm, 8 mm, and 10 mm) consisted of hot-rolled tubes with an outer diameter of d = 219 mm. The minimum distance (gap) between the outer surfaces along the surface of the chord member was g = 51 mm. The member sizes of all tubular K-joint specimens under consideration are listed in Table 1.

The outer diameter of the chord and brace sections of the tested CFST K-joint specimens were the same as those adopted in the CFST trusses of certain arch bridges built in China [30]. For instance, the diameter and thickness of the four chord sections and the braces of the CFST arch trusses in the Nan-pu Bridge (a tie-arch bridge with a span of 312 m located in Chunan, Zhejian Province) are d_0 =550 mm, t_0= 8 mm, d= 219 mm, and t= 8 mm, respectively. In addition, the chord and brace sections of the CFST arch trusses of the Shin-tan-xi Bridge (a half-through arch bridge with a clear span of 136 m located in Fujian Province) have the same sizes as those of the Nan-pu Bridge.

The tensile strength and elongation at failure (based on tensile tests) of the steel in the chord and brace members of the joint specimens under consideration are listed in Table 2. The elastic modulus was 200 GPa. Chord filling with concrete was carried out after positioning the CFST K-joint specimen on the base with its chord in the vertical position. Fresh concrete with a high workability was poured in from the chord top. The workability of the concrete mix was the same as that of concretes usually pumped into the chords of real CFST bridges. The slump class (according to the European Standard EN 206 [35]) was S5. To attain a bond between the concrete and the interior surface of the chord section as well as with the studs welded on it, the concrete was compacted by inducing vibrations in the chord tube through hitting its external surface with a wood hammer.

Table 2. Yield strength, ultimate strength, and elongation at failure of the steel of chord and brace members of the K-joint specimens under consideration.

Type of tubular member and its wall thickness	f_y (MPa)	f_u (MPa)	ε_f
Brace t = 6 mm	330	485	21%
Brace t = 8 mm	325	490	22%
Brace t = 10 mm	322	487	21%
Chord t_0 = 10 mm	311	425	33%

The high chord diameter of 550 mm eased the concrete compaction. The cubic compressive strength and elastic modulus of the adopted concrete were 45 MPa and 33.5 GPa, respectively.

An appropriate device for testing the K-joints was specifically designed and built with the chord and brace members lying in a vertical plane (Fig. 2). A hydraulic jack with a 5000-kN capacity provided a compression force N_{0Ed} at the top of the chord. The chord was fixed to a bearing base at the bottom end and flanged to the jack at the top end. Tension and compression forces were applied to the upper and lower braces, respectively, and were provided by two additional hydraulic jacks (each with a 3000-kN capacity) working against a reaction wall.

The jacks were tied to a beam to prevent the braces from being loaded by the self-weight of the jacks. Jacks and brace members were hinged in the plane of chord and braces, and fixed in the direction orthogonal to this plane. Moreover, transverse displacements of the loaded end of the compression brace in the plane of chord and brace were prevented through providing restraint in the transverse direction, thus preventing the effects of secondary moments at the connected end.

Since K-joints with such size are especially used in arch trusses whose chords are in general in compression, the chord was preloaded with an axial compression force before testing the joint.

The chord of the CFST joint specimens and that of CHS joint specimens were preloaded, respectively, to 4800 kN in three substeps, and to 2500 kN in two substeps. As a result, before

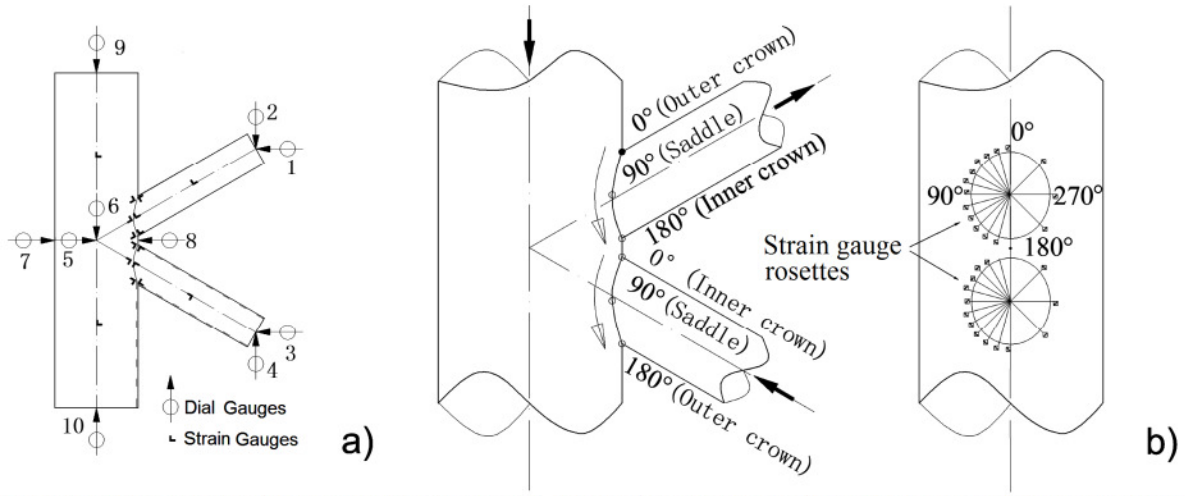

Fig. 3: Instrumentation for measurements (a) and detail of the position of the strain gauge rosettes along the weld toe (b).

loading the braces, the initial stress σ_{0Ed} in the chord tube of both the CFST K-joints and CHS K-joints was much lower than the yield strength of the steel of the chord section. By keeping the axial load in the chord constant, the axial load in the brace members was increased by initial load steps of 20 kN until the deformation was linear. Each load step was subsequently reduced to 10 kN when nonlinear deformations occurred. Finally, a further reduction to 5 kN was applied close to failure. All load steps had a 120-s duration. While the hydraulic jack continuously provided a constant axial force in the chord (as detected by the strain gauges placed at the chord section distant $l_0/4$ from the upper end of the chord), the application of the brace loading decreased the axial force in the chord sections below the joint (as detected by the strain gauges distant $l_0/4$ from the lower end of the chord).

The brace deformations were determined by measuring the vertical and horizontal displacements using dial gauges positioned at the brace ends and on the chord surface where the chord and brace centrelines met (Fig. 3). *The strains along the welded connection of chord and brace members were determined via multi-axial strain gauges (strain gauge rosettes). Figure 3b illustrates the scheme of their position close to the weld toe.* Also, uniaxial strain gauges were positioned at mid-length of brace and chord members, besides at $l_0/4$ from the upper and lower ends of the chord (Figure 3a).

3. CHS and CFST K-joint experimental results and discussion

The failure modes of CHS joints have been studied by organizations as CIDECT [33,36], IIW [34], API [37]. Updated guidelines for their design and analysis are now available in the international standard ISO 14346 [38], that provides capacity equations for axially loaded K gap joints (as well as for T and X joints) with updated strength functions [39]. By proposing corrections of the Eurocode 3-Part 1-8, Section 7 "Hollow Section Joints", Van der Vegte and Wardenier [40] considered that while modifications of chord stress functions of the Eurocode 3 are really necessary for chord tension loading, no changes are needed for chord compression loading (that is the case of the K-joints herein considered).

Both the American Welding Society (AWS) code [31] and the Eurocode 3 [32] provide formulations to check the resistance of CHS joints. The Eurocode 3 lists the following failure modes: chord face failure (chord face plastification), chord shear failure, punching shear failure of the chord wall (crack initiation leading to rupture of the brace members from the chord member), local buckling failure of a brace member or of a chord member at the joint location, and brace failure with reduced effective width (cracking in the welds or in the brace members). In addition to the definition of the different failure modes, design regulations for CHS joints are proposed in both the AWS code and the Eurocode 3 [31, 32].

The behaviour of CFST tubular joints is less studied, and none of the codes provide specific formulations to evaluate their resistance. Because the in-filled concrete does not permit any failure mode with inward deformation of the chord (i.e., local buckling of the chord in the joint location, chord cross-sectional failure, and chord shear failure, that could only occur for high values of the ratio $\beta=d/d_0$)), many failure modes typical of CHS K-joints need not be considered in the analysis of CFST joints, thus simplifying their design.

Therefore, filling the chord with concrete results in a stiffening effect in the CFST joints compared to CHS joints, as well as in a more uniform strain distribution at the joint location in the chord and in the brace ends.

For instance, Fig. 4 shows that for the same axial force in the brace, the distribution of the principal strains along the toe of the welded connection between the chord and the brace members of CFST joints (Figures 4b) was significantly more uniform and with lower peak values than that in CHS joints with the same geometry (Figures 4a).

The CFST joints can be further stiffened by the addition of studs welded to the interior surface of the chord in the joint region. Through the addition of studs, the chord section is better constrained by the in-filled concrete and its deformation is therefore reduced.

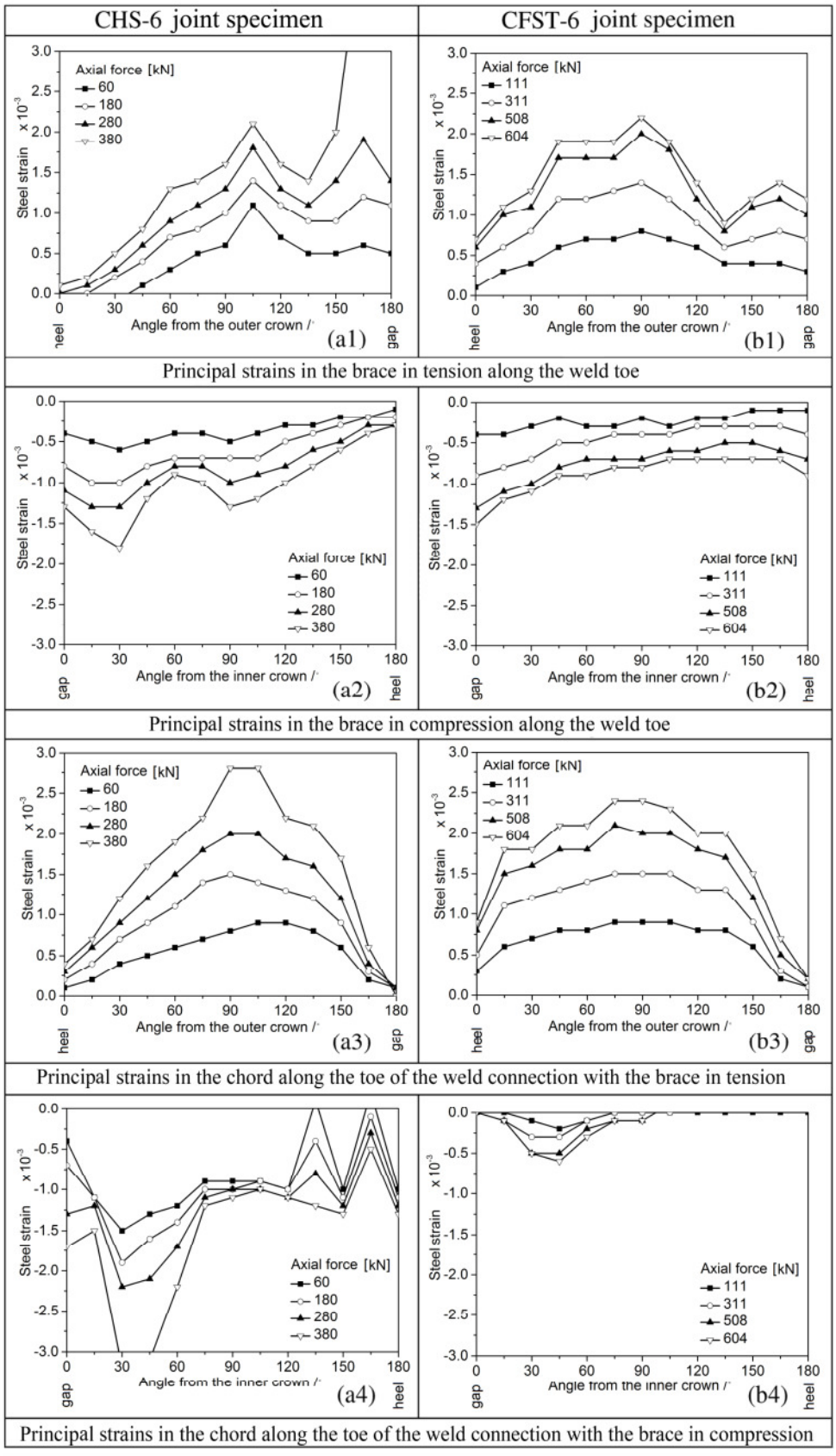

Fig.4. Principal strains along the weld toe of specimens CHS-6 and CFST-6

1

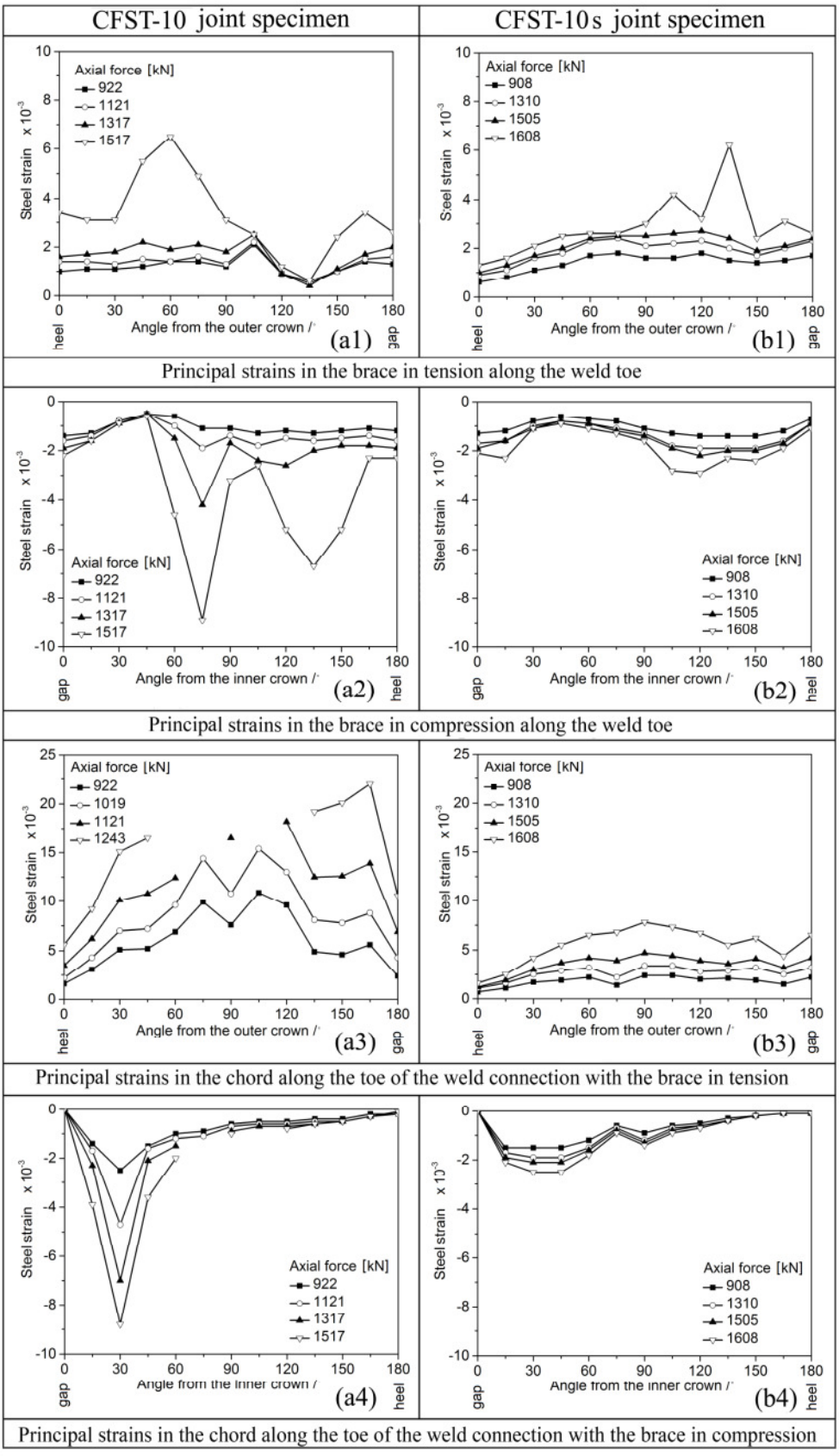

Fig.5. Principal strains along the weld toe of specimens CFST-10 and CFST-10s

1

Therefore, the studs are able to further reduce peaks and non-uniformity of the strain distribution at the joint location in the chord and the brace members of CFST specimens with studs compared to those in CFST specimens without studs, as shown in the comparison between the diagrams of Figures 5a with those of Figures 5b.

Finally, when the axial force in the braces was applied, the CFST chord was subjected to lateral local compression in the connection area with the compression brace. With reference to the strength prediction method described by Hou, Han and Zhao [23], checking the CFST chord subjected to lateral bearing force, the predicted ultimate strength was N_{uc}= 6980 kN, where:

$$N_{uc} = 2 f_{ck} \frac{A_1}{\sin\theta} \sqrt{A_2 / A_1}$$

with $A_1 = \pi d_1/4$ and $A_2 = A_1/\sin\theta + 2\, d_0 d_1$, and was much higher than the maximum compression force in the brace of the specimens under consideration (See Tables 3 and 4). Actually, he concrete in the chord beneath the connection area was not crushed.

Sections 3.1 and 3.2 discuss in detail the test results and the consequent joint design procedure.

3.1. CHS K-joint tests

Two CHS K-joint specimens (CHS-6 and CHS-8) with brace members with wall thicknesses of t = 6 mm and 8 mm, respectively, were tested. Only punching shear and chord face failure modes were considered because the joint geometry was within the range of validity of the Eurocode 3 on CHS K-joints [32] for which no other failure mode must be considered, namely:

$$0.2 < d/d_0 < 1; \quad 2t \leqslant g; \quad \text{Class 2 and } 10 < d_0/t_0 < 50; \quad \text{Class 2 and } 10 < d/t < 50 \qquad (1)$$

According to the Eurocode 3, the tubular sections of the chord and the braces with t = 6 mm of the K-joint specimens under consideration were classified as Class 2, while the brace sections with t = 8 and 10 mm were classified as Class 1.

Therefore, joint resistance was calculated through the formulae of both the AWS code and the

Eurocode 3 for these two failure modes only (Table 3) [31-32].

Consider the formulae of the Eurocode 3 [31] in which the yield strength of the chord steel f_{y0} is, in general, different from that of the brace steel. The joint resistance for the chord face failure mode of the joint of the compression brace is expressed as:

$$N_{Rd} = \frac{k_g\, k_p\, f_{y0}\, t_0{}^2\, (1.8 + 10.2\, d/d_0)}{\sin\theta\, \gamma_{M5}} \tag{2}$$

where:

$$k_g = \gamma^{0.2}\left[1 + \frac{0.024\gamma^{1.2}}{1 + e^{(0.5g/t_0 - 1.33)}}\right] \tag{3}$$

$$k_p = \begin{cases} 1 - 0.3\, n_p\, (1 + n_p) & \text{for compression chords} \\ 1 & \text{for tension chords} \end{cases} \tag{4}$$

and where g is the gap, $\gamma = d_0/(2\, t_0)$, $n_p = \sigma_{0Ed} / f_{y0}$, and $\gamma_{M5} = 1$.

To calculate the joint resistance with the punching shear failure mode, the Eurocode 3 proposes the formula:

$$N_{Rd} = \frac{f_{y0}}{\sqrt{3}}\, t_0 \pi\, d\, \frac{(1 + \sin\theta)}{2\sin^2\theta} \,/\gamma_{M5} \tag{5}$$

with the restriction that $d \le d_0 - 2t_0$.

Similarly, according to the corresponding formulations of the Load and Resistance Factor Design (LFRD) format of the AWS code [32], the ultimate force of the chord face failure mode is:

$$P_u = \frac{t_0^2\, f_{y0}}{sin\theta}(6\pi\beta) Q_q Q_f \tag{6}$$

where after defining the coefficients $\alpha = 1 - 0.7\, g/d$, $\beta = d/d_0$, and $\gamma = d_0/2t_0$, Q_q and Q_f are expressed as:

$$Q_f = 1 - \lambda\, \gamma \bar{U}^2 \qquad Q_q = \left(\frac{1.7}{\alpha} + \frac{0.18}{\beta}\right) Q_\beta^{0.7(\alpha - 1)} \tag{7}$$

with $Q_\beta = 0.3/[\beta\,(1 - 0.8333\,\beta)]$ for $\beta > 0.6$ (otherwise $Q_\beta = 1$) and where, for brace members

subjected to axial load only, $\overline{U}^2$ is the square of the ratio of actual stress in the chord member due to the axial load over the allowable stress, and $\lambda = 0.030$.

Additionally, the AWS formulation for the punching shear failure mode is:

$$P_u = \frac{\pi d t_0}{sin\theta} \frac{f_{y0}}{\sqrt{3}} \quad (8)$$

The experimental tests showed that the chord face failure mode occurred in both CHS K-joint specimens (Fig. 6), in accordance with the fact that using the above formulations, the joint resistance to punching shear was much higher than that for the chord face failure mode (Table 3). *Moreover, when in both the CHS-6 and CHS-8 specimens the joint resistance for chord face failure was attained (717 kN and 719 kN, respectively, see Table 3) with high plastic deformations (Fig. 7), the typical peak of strain in the tension brace at the crown toe (for 180°=gap in Fig. 4-a1) caused the formation of a crack (see the upper brace of Fig. 6) whose rapid propagation led the joint to fail suddenly.*

It can be noted that when this crack propagated, the chord face failure mode already occurred, with the compression force in the brace practically constant, but with the ultimate deformation of the compression brace that was still quite small, being slightly smaller than 5 mm (Fig. 7). *The inward deformation at the chord face was therefore much lower than Lu's deformation limit of 3%d_0 = 15.3 mm [40]. Fig. 4a-4 shows that, however, in specimen CHS-6 the principal strains in the chord along the toe of the welded connection with the compression brace were much higher (and with a pronounced peak of strain at an angle of 40° from the crown heel) than those along the toe of the*

Table 3. Resistance values obtained from testing and from the formulae of the AWS code and the Eurocode 3 for the CHS K-joint specimens under consideration. The results in bold are referred to the actual failure mode.

Specimen	Failure mode	Joint resistance by testing (kN)	Brace yield strength (kN)	Calculated values of joint resistance obtained by means of the formulae of the Eurocode 3 (EC-3) and the AWS code (kN)				Ratio between test and-calculated joint resistance	
				Chord face failure mode		Punching shear failure mode			
				AWS	EC-3	AWS	EC-3	AWS	EC-3
CHS-6	Chord face failure	**717**	1324	**478**	**417**	1426	1536	**150%**	**172%**
CHS-8		**719**	1723	**478**	**417**	1426	1536	**150%**	**172%**

chord of specimen CFST-6 (Fig. 4b-4), the latter being limited by the stiffening effect of the concrete infilling of the chord. This stiffening effect was of course practically ineffective along the weld connection with the tension brace, where the principal strains along the toe in the CFST chord (Fig. 4b-3) were only slightly lower than those in the CHS chord (Fig. 4a-3).

It can be noted that when the peak of strain (see Fig. 4-a1, 180° = gap) led to crack initiation in the tension brace (Fig.6) at the crown toe (with joint resistance for chord face failure already attained), the axial force in the braces of specimens CHS-6 and CHS-8 (717 - 719 kN, respectively) was however much lower than their brace yield strength $N_R = \pi(d-t)\,t \cdot f_y$ *(1324 kN and 1723 kN,*

Fig. 6. Chord face failure mode of the CHS K-joint specimens CHS-6 (a) and CHS-8 (b)

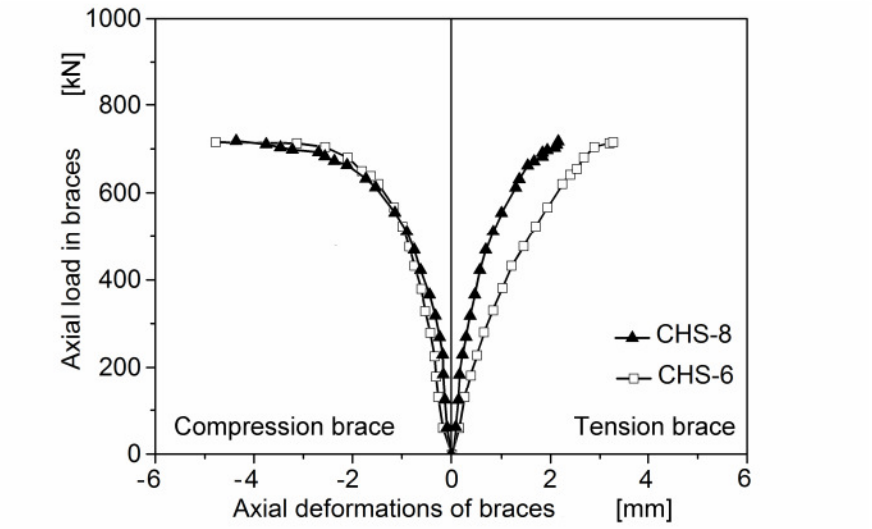

Fig. 7. Axial Load versus Axial Deformation diagram of the braces of the joint specimens CHS-6 and CHS-8, both failed via the chord face failure mode.

respectively). In fact, for the typical non-uniform strain distribution along the weld connection of tubular joints, principal strains of only 1.6 × 10^{-3} strains (coinciding with the yield strain of the steel brace and therefore corresponding to its yield strength of 320 MPa) were easily attained even for low values of the brace axial force (see Fig. 4). For instance, Fig. 4-a1 shows that the peak of strain in the brace along the weld connection at an angle of 165 ° (that is close to the gap location) was almost 2 × 10^{-3} strains (thus higher than steel yield strain) for a tension force in the brace of only 280 kN.

The experimental results show that the resistances for chord face failure of the two specimens CHS-6 and CHS-8 (717 kN and 719 kN, respectively) did not depend on the brace wall thicknesses of 6 mm and 8 mm, in accordance with the two formulations of the AWS code and the Eurocode 3 on joint resistance for chord face failure [31-32], which are both independent of brace wall thickness.

Table 3 summarises the comparison between experimental results and the theoretical values obtained from both the Eurocode 3 and AWS codes. The occurrence of the chord face failure mode was expected according to the EC3 and AWS, for which the calculated resistance to punching shear failure was greater than the chord face failure values. *Table 3 also shows that the formulations of both codes (originally derived by the ring model that only considered chord plastification [36,41]) resulted in rather conservative values. In fact, the results of the formula of the Eurocode 3 and of the AWS code exceeded the resistance value obtained by testing at 72% and 50%, respectively. This was likely due to the large fillet welds (whose leg length was twice the brace wall thickness) that significantly reduced the effective gap size between the braces.*

3.2. CFST K-joint tests

In testing of the CFST K-joints, two types of failure modes were observed. A member failure mode occurred in the compression brace of the specimen CFST-6 (t = 6 mm), while the specimens CFST-8 and CFST-10 (t = 8 and 10 mm, respectively) failed for punching shear. Brace failure was caused

by yielding at the joint location, with an outward bulge that formed close to the joint (Fig. 8). The compression force at failure was 1115 kN (Table 4 and Fig. 9), which was less than the brace yield strength of 1325 kN. *Yielding at the brace end was favoured by the extremes in the strain distribution (as expected in a tubular joint) along the welded connection between chord and compression brace (Fig.4-a2).*

Brace buckling could not occur before brace failure. In fact, even assuming that the brace length was 1000 mm (instead of 900 mm) and that the braces were hinged at their ends (although end rotation was not completely allowed by the welded connection), the brace could not buckle before because it was too short with respect to the diameter d = 219 mm and the wall thickness t = 6 mm of the brace. In fact, in checking the buckling resistance of the compression brace according to the Eurocode 3, the calculated value of the buckling coefficient χ was 1, meaning that no overall buckling of the brace could occur.

According to the AWS code [32], the inequality $d/t = 36.5 < (3300 \times 6.9 \text{ MPa}/f_y) = 69$ (for which local buckling at the joint location in the compression brace of a CHS joint is prevented) was satisfied, meaning that local buckling was therefore prevented further in the compression brace of the CFST joint, because of the lower strain level under the same loading of the latter with respect to

(a) Bulge at the end of the compression brace of specimen CFST-6

(b) Shear lines on the surface of the compression brace of specimen CFST-6

(c) Bulge at the end of the compression brace of specimen CFST-6s

Fig. 8. Member failure mode for yielding of the compression brace of the K-joint specimens CFST-6 and CFST-6s with wall thickness t = 6 mm.

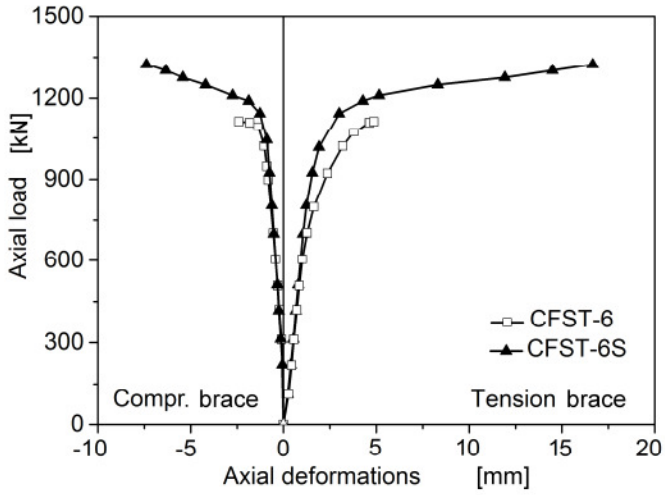

Fig. 9. Comparison between the Axial Load versus Axial Deformation diagrams of the compression braces failed for yielding of the specimens CFST-6 and CFST-6s.

the former.

In fact, the concrete filling of the chord reduced the deformation of the joint, thus reducing the non-uniformity of the strain distribution with respect to a similar CHS joint (compare Figures 4a with 4b). Hence, since on one hand the joint geometry was within the range of validity of the Eurocode 3 for which only chord face failure and punching shear failure of CHS joints should be considered, and on the other hand the concrete filling of the chord did not allow all failure modes typical of CHS K-joints with inward deformation of the chord, then the chord face failure mode was not expected, while only the punching shear failure mode could occur, unless any brace failure mode

(a) CFST-8 (b) CFST-10 (c) CFST-8s (d) CFST-10s

Fig. 10. CFST K-joint specimens failed in punching shear without studs (a,b) and with studs (b,c).

occurred before.

In fact, in testing specimens CFST-8 and CFST-10, punching shear failure was observed (Fig. 10a, 10b). It is to be considered a typical failure mode of CFST K-joints.

The values of punching shear resistance obtained from testing were higher than the resistance values obtained from the formulae of the AWS code [31] and the Eurocode 3 [32] on CHS K-joints, but were closer to the values obtained from the formula of the latter code.

The experimental results show that for the two K-joint specimens CFST-8 and CFST-10 (t = 8 mm and 10 mm), the resistances to punching shear were 1541 kN and 1612 kN, respectively (Table 4 and Fig. 11). These results are quite similar, and therefore independent of t, as expected.

Similar results were also obtained by Huang et al. [29] in testing of three CFST truss girders (size of brace and chord sections d = 48 mm, t = 1.5 mm, and d_0 = 89 mm, t_0 = 1.8 mm, respectively; girder total height and span length 488 and 2880 mm, respectively; steel with f_y=428 MPa and f_u=533 MPa; concrete infilling of the chords with f_c=38.6 MPa), whose joints connecting the most heavily loaded tension brace with the compression chord failed by punching shear. The punching shear resistance of their CFST joints (that can be accounted as small scale joints compared to those herein considered) was 96, 99 and 92 kN, while the ratios between joint resistance obtained by

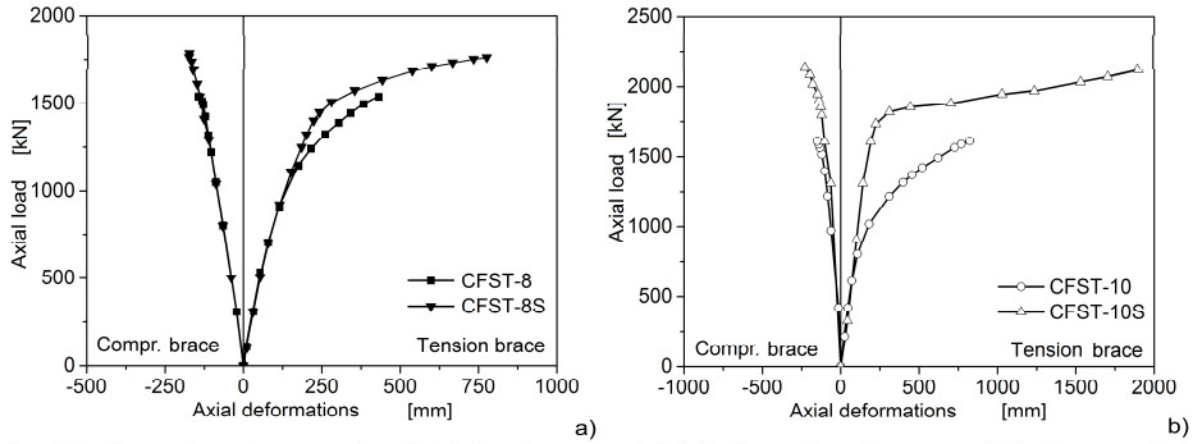

Fig. 11. Comparison between the Axial Load versus Axial Deformation diagrams of the braces of the specimens CFST-8 and CFST-10 with those of the specimens CFST-8s and CFST-10s, which all failed via the punching shear failure mode.

Table 4. Resistance values obtained from testing and from the formulae of the AWS code and the Eurocode 3 for CFST K-joint specimens under consideration with and without studs. The results in bold are referred to the actual failure mode.

Specimen	Failure mode	Joint resistance by testing (kN)	Brace yield strength (kN)	Calculated values of joint resistance (kN) Punching shear failure mode		Ratio between test and-calculated joint resistance	
				AWS	EC-3	AWS	EC-3
CFST-6	Brace failure	**1115**	**1324**	1426	1536		
CFST-8	Punching shear failure	**1541**	1723	**1426**	**1536**	**108%**	**100%**
CFST-10		**1612**	2113	**1426**	**1536**	**113%**	**105%**
CFST-6s *	Brace failure	**1323**	**1324**	1426	1536		
CFST-8s *	Punching shear + brace failure	**1790**	**1723**	**1426**	**1536**	**126%**	**117%**
CFST-10s *		**2134**	**2113**	**1426**	**1536**	**150%**	**139%**

*s = with studs

testing and calculated through the AWS code and the Eurocode 3 were, respectively: 117, 121, 112% and 105, 108, 101%.

Therefore, the formula of the Eurocode 3 seems to predict with sufficient accuracy not only the punching shear resistance obtained by testing the large scale CFST joints herein considered, but also that of small scale joints obtained by testing the above CFST truss girders. Because no specific formulations are available in the codes to check CFST joints against punching shear failure, it seems to be reasonable to use the formula of the Eurocode 3 for the resistance to punching shear of CHS K-joints also for CFST K-joints.

Table 4 summarises the results obtained for the three CFST K-joints in the range of validity of the Eurocode 3 considered herein. It shows that brace failure occurred in the CFST specimen CFST-6 for which brace yield strength was lower than joint resistance to punching shear, whereas the punching shear failure mode occurred in CFST-8 and CFST-10 specimens (for which the brace yield strengths of 1723 kN and 2113 kN, respectively, were higher than the joint resistance to punching shear).

Table 4 also shows that both the formulae of the Eurocode 3 and that of the AWS code well estimated the joint resistance to punching shear, but the former formula better fit the experimental results, because produced about the same values of joint resistance obtained by testing (differing at most by 5%).

3.3. Improving the behaviour of CFST K-joint specimens by adding studs welded to the interior surface of the chord tube

Finally, three CFST K-joint specimens with studs welded to the interior surface of the chord across the joint region were tested (Fig. 12). The three specimens (CFST-6s, CFST-8s, CFST-10s) differed from each other only in the brace wall thicknesses of 6 mm, 8 mm and 10 mm, respectively, and studs with a height of 80 mm were used (shank diameter = 19 mm, head diameter = 32 mm, head thickness = 12 mm). The stud spacing in the direction of the chord tube was 150 mm, and spacing

Fig. 12. View of the interior surface of the chord tube of a CFST joint with studs

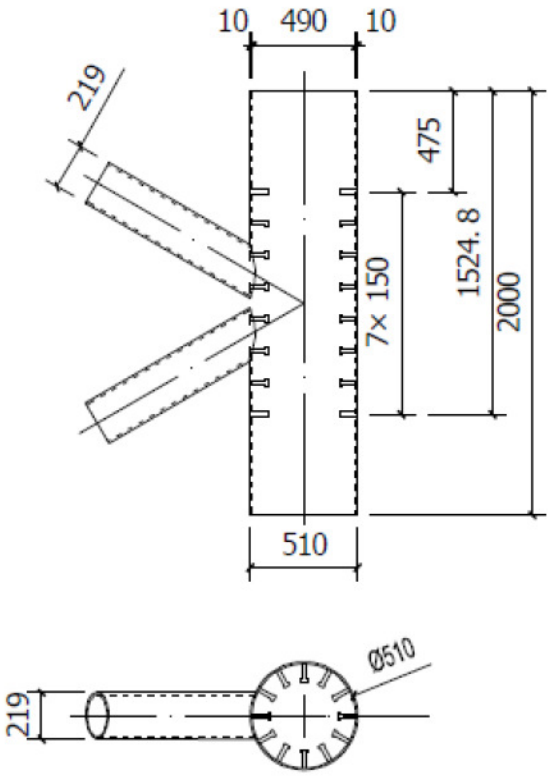

Fig. 13. Stud arrangement of the CFST joints with studs

along the interior circumference of each chord section was 128 mm (12 studs per section). Because spacing in the longitudinal direction was 150 mm and the studs were welded on eight circular sections of the chord tube, therefore, in each joint, 96 studs were welded along 1050 mm in length across the joint region via manual DC welding (Fig.13). The weld quality was verified by means of pull tests and bend tests, according to the qualification requirements of the stud-welding section of the AWS code [31].

All three CFST K-joint specimens with studs failed in the same failure modes of the corresponding specimens without studs (Figures 8c, 10c and 10d), but the resistance and ultimate deformation of the former specimens were always greater than those of the latter.

In testing specimen CFST-6s, the member failure mode occurred via yielding of the compression brace with a compressive force of 1323 kN. The brace yield strength of 1325 kN was attained with a bulge forming at the connected end of the compression brace (Fig. 8c). A comparison between the axial load versus axial deformation diagrams of the compression braces of specimens CFST-6 and CFST-6s shows that the effect of the studs welded to the interior chord face in the joint region mainly resulted in a higher ultimate deformation of the brace (Fig. 9). *Moreover, by comparing Figures 5a-2 and 5a-4 with, respectively, Figures 5b-2 and 5b-4, it can be noted how stud addition resulted in a lower level of strains in the chord and in the compression brace along the weld toe, without sharp peaks of strain (as that occurring at an angle of 30° from the gap of the CFST chord without studs in Fig. 5a-4) and with more uniform strain distribution.*

Similarly to the corresponding specimens without studs, specimens CFST-8s and CFST-10s failed by punching shear. *The addition of studs was shown to increase joint resistance (Fig. 11 and Table 4) and caused a general reduction of strain level in the whole joint for the same loading, particularly in the chord (compare Figure 5-a3 and 5-b3, where, for same tension force in the brace, the maximum principal strain in the chord of specimen CFST 10 was much higher than that in the chord of specimen CFST 10s). Studs better involved concrete in the chord deformation at the*

joint location, thus reducing strains in the chord face. Through reducing strain level, the addition of studs delayed the cracking of the chord along the welded connection with the tension brace.

Moreover, the delay of the chord cracking before punching shear failure provided an important improvement in terms of ultimate deformation of the of the K-joint specimens with studs (778 and 1900 mm for specimens CFST-8s and CFST-10s, respectively) compared to that of the corresponding K-joint specimens without studs (358 and 823 mm for specimens CFST-8 and CFST-10, respectively), see Fig. 11. The addition of studs thus resulted in doubling the ultimate deformation, and in significantly increasing CFST joint resistance to punching shear.

The experimental results show that, for the CFST joint specimens with studs, the resistance to punching shear was so significantly increased (compared to that of the corresponding specimens without studs and to the resistance value expected from the formulations of the Eurocode 3 and the AWS code) that brace yield strength was attained. Nevertheless, Figures 10c and 10d show that joints CFST-8s and CFST-10s failed for punching shear, with a crack propagating in the chord close to the weld toe just when the brace axial force reached brace yield strength.

However, additional research on the behaviour of CFST K-joints with studs appears to be necessary.

4. Conclusions

The increasing use of CFST truss structures, especially in certain countries (i.e., in China), requires a deeper knowledge of their behaviour. The objective of this article was an experimental investigation of the failure modes and resistance of CFST K-joint specimens whose size was on the same scale as that of joints and members of the tubular structures used in real bridges. Additionally, after testing CHS K-joints with the same size, the behaviour of CFST and CHS K-joints was compared. The improved behaviour and resistance increases provided by the addition of studs welded to the interior face of the chord of CFST K-joints were also investigated.

Although the CHS K-joints failed by chord face plastification (a frequent failure mode of CHS K-joints), two of the three CFST K-joints failed by punching shear, a typical failure mode of CFST K-joints that occurs unless any brace failure mode occurs before, as occurred in the CFST K-joint specimens (both with and without studs) with smaller wall thickness of 6 mm.

The test results on CFST K-joint specimens showed that resistance to punching shear calculated from the formula for CHS K-joints in the Eurocode 3 was close to (although always less than) the actual resistance of CFST K-joints obtained by testing. Therefore, it appears reasonable to design CFST K-joints using the formula of the Eurocode 3, provided that the K-joints are within the required range of validity for the joint geometry. The AWS code also could be used, but more conservative resistance values would be obtained.

Therefore, in designing CFST K-joints, the joint resistance can be identified as the lowest value between the resistance to punching shear failure (i.e., calculated by means of the previously mentioned formula of the Eurocode 3) and the brace resistance against any brace failure mode.

Finally, the effect on the CFST joint resistance of welding studs to the chord interior face was investigated. In addition to the in-filled concrete, stud addition was shown to produce a further increase in the joint stiffness and a reduction of the strain level in CFST K-joints such that both the resistance and ultimate deformation of the CFST joint were significantly increased. Nevertheless, further investigations are necessary to predict the resistance increase of CFST K-joints caused by stud addition.

Acknowledgements

The Authors thank the Laboratory Technicians of the Structural Lab of the College of Civil Engineering of the University of Fuzhou for their fundamental collaboration in carrying out this experimental research.

This research was supported by the National Science Founding of China through the granted program N. 50578042 and N. 51008079.

The role of the Siberc (Sustainable and Innovative Bridges Engineering Research Center, Fujian Province Universities - China), and of the RAS (Sardinian Region – Italy), in supporting this joint research between the University of Fuzhou and the University of Cagliari is also acknowledged.

References

[1] Chen B. An overview of concrete and CFST arch bridges in China. In: Proc. of the 5th Int. Conf. on Arch Bridges "Arch'07", Madeira, Portugal, invited lecture, Multicomp, Lda. 2007. p. 29-44.

[2] Chen B, Wang T-L. Overview of concrete filled steel tube arch bridges in China. Practice periodical on structural design and construction, ASCE. 2009; 14(2): 70-80.

[3] Han L-H. Some recent developments of concrete filled steel tubular (CFST) structures in China. In: Proc. of the 4th Int. Conf. on Steel & Composite Structures 2010; 21-23 July, Sydney, Australia; 2010. p. 43-54.

[4] Wu Q, Yoshimura M, Takahashi K, Nakamura S, Nakamura T. Nonlinear seismic properties of the Second Saikai Bridge: A concrete filled tubular (CFT) arch bridge. Eng. Str. 2006. 28(2): 163-82

[5] NSEL Report 008. A Synopsis of Studies of the Monotonic and Cyclic Behavior of Concrete-Filled Steel Tube Members, Connections, and Frames. NSEL Report Series, Report No. NSEL-008; April 2008.

[6] Zhang Lianyan, Li Zesheng, Cheng Maofang. Concrete-filled steel tubular truss girders as bridge structures. People communication Press. Beijing. 2000. (in Chinese)

[7] Han L, Zheng L, He S, , Tao Z. Tests on curved concrete filled steel tubular members subjected to axial compression. J Const Steel Res. 2011. 67(6) *965-976.*

[8] Xue J-Q, Briseghella B, Chen B. Effects of debonding on circular CFST stub columns. J Const Steel Res. 2011, 69(1), 64-76.

[9] Han L-H. Concrete-filled steel tube structures-theory and design. 2nd ed. Beijing: Science Press; 2007.

[10] Wardenier J. Hollow sections in structural applications. CIDECT Comité International pour le Développement et l'Etude de la Construction Tubulaire, 2001.

[11] Wardenier J, Kurobane Y, Packer J A, Dutta D, Yeomans N. Design guide for circular hollow section (CHS) joints under predominantly static loading. 1st ed. Cologne (Germany): Verlag TüV Rheinland; 1991.

[12] Packer JA, Henderson J E. Hollow structural section connections and trusses-a design guide. 2nd ed. Toronto (Ont., Canada): Canadian Institute of Steel Construction; 1997.

[13] Qian XD, Choo YS, Liew JY R, et al. Simulation of Ductile Fracture of Circular Hollow Section Joints Using the Gurson Model. J Str Eng. ASCE 2005; 131(5): 768-80.

[14] Tebbett IE, Beckett CD, Billington CJ. The punching shear strength of tubular joints reinforced with a grouted pile. In: Proc. of offshore technology conference, offshore technology conference association. Houston, Texas: 1979. p. 915-21.

[15] Packer JA, Fear CE. Concrete-filled rectangular hollow section X and T connections. In: Proc. of the 4-th Int. Symp. on Tubular Structures, Delft (The Netherlands), 1991. p. 382-91.

[16] Kenedi WW, Packer JA. Concrete-Filled Hollow Structural Section T- and K-Joints. CIDECT Report No. 5AV-13/91. University of Toronto, Canada. 1991.

[17] Packer, JA, Henderson, IE. Design criteria for concrete-filled HSS joints. CIDECT Report No. 5AV- 26/92, University of Toronto, Toronto, Canada. 1992.

[18] Packer JA. Concrete filled HSS connections. J Str Eng. ASCE 1995, 121(3): 458-467.

[19] Feng R, Young B. Tests of concrete-filled stainless steel tubular T-joints. J Const Steel Res. 2008, 64(11): 1283-93.

[20] Han Q, Lu Y, Yu B, Yin Y. Ultimate Load Capacity and Reinforcement of Circular-Hollow-Section N-Joint. Transaction of Tainjin University, 2010, 16(1): 1-5.

[21] Zheng W, Liu X, Zhang B, Zhang G. Experimental research on ultimate bearing capacity of grouted-round-steel-tube N-joint. Journal of Harbin Institute of Technology, 2007, 14(3): 322-29.

[22] Chen Z. Static strength of tubular X-joint with chord fully infilled with high strength grout Doctorate degree thesis. National University of Singapore, Singapore. 2010.

[23] Hou C, Han L-H, ZhaoX-L. Concrete-filled circular steel tubes subjected to local bearing force: Experiments. J Const Steel Res. 2013: 83, 90-104.

[24] Hou C, Han L-H, ZhaoX-L. Concrete-filled circular steel tubes subjected to local bearing force: Finite element analysis. Thin-Walled Structures, 2014, 77: 109-119

[25] Sakai Y, Hosaka T, Isoe A, Ichikawa A, Mitsuki K. Experiments on concrete filled and reinforced tubular K-joints of truss girder. J Const Steel Res. 2004, 60(3): 683-99.

[26] Xu W, Han L-H, Tao Z. Flexural behaviour of curved concrete filled steel tubular trusses. J of Const Steel Res. 2014, 93: 119–134.

[27] Huang W. Ultimate bearing capacity of concrete filled steel tubular truss girders. Doctorate degree thesis. Fuzhou University, Fuzhou, China. 2009. (In Chinese)

[28] Huang W, Chen B. Research on influence of web member on mechanical behavior of CFST Truss Girders. China J Build Stru, 2009, 30(1): 55-61. (in Chinese).

[29] Huang W, Fenu L, Chen B, Liu J, Briseghella B. Resistance of Welded Joints of Concrete-Filled Steel Tubular Truss Girders. In: Proc. of the 10th Int. Conf. on Advances in Steel Concrete Composite and Hybrid Structures (ASCCS 2012). Singapore, July 2-4, 2012.

[30] Chen B, Radic J. Construction of arch bridges. Proc. of the 2-nd Chinese-Croatian Joint Colloquium. Fuzhou, October 5-9, 2009.

[31] CEN. Eurocode 3: Design of steel structures, part 1.8: Design of joints. European Committee for Standardization. EN 1993-1-8, CEN. Brussels, Belgium, 2007.

[32] American National Standard Institute (ANSI). AWS D1.1/D1.1M:2004: Structural welding code - steel. American Welding Society, Miami (USA). 2004.

[33] Wardenier J, Kurobane Y, Packer JA , van der Vegte GJ, Zhao X-L. Design guide for circular hollow section (CHS) joints under predominantly static loading (2nd ed). CIDECT, Comité International Pour le Développement et L'étude de la Construction Tubulaire. LSS Verlag, 2010.

[34] International Institute of Welding (IIW). IIW static design procedure for welded hollow section joints-Recommendations. IIW Doc. XV-1281-08. In: IIW Annual Assembly, Graz, Austria, 2008.

[35] European Norm EN 206-1, Concrete - Part 1: Specification, performance, production and conformity. Brussels, Belgium, 2000.

[36] Wardenier J, Packer JA, Zhao X-L, van der Vegte GJ. Hollow sections in structural applications, CIDECT, Comité International Pour le Développement et L'étude de la Construction Tubulaire. Bouwen met Staal, The Netherlands, 2010.

[37] API. American Petroleum Institute. Recommended practice for planning, designing and constructing fixed offshore platforms. API RP 2A-LRFD, Washington DC; 1993.

[38] ISO 14346: Static design procedure for welded hollow-section joints – Recommendations. 1st ed., Geneva, Switzerland, 2013,

[39] Van der Vegte GJ, Wardenier J. Evaluation of the recent IIW (2012) and ISO (2013) strength equations for axially loaded CHS K gap joints. Steel Constr. 2014, 7 (2), 97-106.

[40] Wardenier J, Puthli RS, Van der Vegte GJ. Proposed corrections for the 1993-1-8 Part "Hollow Section Joints" , Tubular Stuctures XIV (Edited by Gardner L), CRC Press/Balkema, Leiden, The Netherlands, 2012.

[41] Lu LH. The static strength of I-beam to rectangular hollow section column connections. Dissertation, Promoter: Wardenier J, Faculty of Engineering and Geosciences, Delft University of Technology. Delft University Press, 1997.

[42] ESDEP WG 13: Tubular structures - Lecture 13.2. The Behaviour and Design of Welded Connections between Circular Hollow Sections under Predominantly Static Loading. European Steel Design Education Program. the ESDEP Society, the Steel Construction Institute (UK), 1995.